Interfacing Conjugated Polymers with Magnetic Nanowires

Vincent Callegari and Sophie Demoustier-Champagne*

Institut de la Matière Condensée et des Nanosciences—Bio & Soft Matter (IMCN/BSMA), Université catholique de Louvain, Place Croix du Sud, 1, B-1348 Louvain-La-Neuve, Belgium

ABSTRACT A variety of new multisegmented nanowires based on magnetic metals and conjugated polymers, polypyrrole (PPy) and poly(3,4-ethylenedioxythiophene) (PEDOT), were synthesized by an all-electrochemical template method for precise control over segment lengths. To overcome the major problem occurring when performing direct electrodeposition of PPy or PEDOT on active metals, such as nickel, the concomitant metal oxidation and redissolution at the positive potentials required for polymer formation, we developed a two-step chemical process. Prior to electropolymerization, the Ni surface was pretreated with 3-(pyrrol-1-yl) propanoic acid. This strategy allowed the improvement of the polymer adhesion, resulting in the formation of mechanically robust Ni/conjugated polymer interfaces. By this way, we successfully prepared various original trisegmented nanostructures, such as systems containing one magnetic segment, Ni-PPy-Pt and Ni-PEDOT-Au nanowires, and systems containing two different magnetic metals, Ni-PPy-Co and Ni-PEDOT-Co nanowires. All these one-dimensional multicomponent nanostructures present both fundamental interest and potential applications in nanoelectronics and in biomedical field.

KEYWORDS: electrochemical template synthesis • multisegmented nanowires • conjugated polymers • magnetic metal • organic spintronics.

INTRODUCTION

Because of their unique properties, one-dimensional (1D) nanowires are particularly attractive for sensing and electronics applications. However, to incorporate these nanostructures into devices, it is critically important to be able to control their motion and position. Various approaches for controlling the position and alignment of nanowires or nanotubes have already been reported. Among them, the use of chemically patterned prefabricated electrodes (1) and the use of electrical or magnetic fields (2) are particularly developed. For performing such a type of nanowire manipulation, the nanostructures must generally contain an appropriate material different from the functional one. For that reason, the design and synthesis of multicomponent 1D nanostructures, containing different materials that can perform specific functions, have recently received considerable attention (3−12). An attractive route for preparing multisegmented nanowires involves sequential electrodeposition into a nanoporous membrane, followed by the dissolution of the nanoporous template. However, one of the major issue for the application of multicomponent nanowires is the improvement of the mechanical strength of the different in-wire material interfaces, this problem being even more marked in narrow ($\Phi < 120$ nm) diameter nanowires. Recently, we reported on an effective all-electrochemical template-based method for preparing a variety of well-shaped and mechanically robust tri- and tetra-segmented noble metal (Au or Pt)-conjugated polymer (PPy and PEDOT) nanowires (13, 14). In the present work, we aimed at developing a method allowing the preparation of magnetic metal (Ni or Co)-conjugated polymer (CP) based nanowires. The electropolymerization of pyrrole or 3,4-ethylenedioxythiophene on active metals is much more difficult than on noble metals. Indeed, the oxidation potentials of these metals are much lower than that of the conjugated monomers and, consequently, dissolution of the metal occurs before electropolymerization begins. To form homogeneous and adherent conjugated polymer layers onto oxidizable metals, it is thus necessary to find synthesis conditions that will strongly passivate the metal without impeding electropolymerization. Though, there is an extensive literature on the electropolymerization of conducting polymers on oxidizable metals, there are very few reports devoted to deposition on nickel (15−17), and none on the synthesis of Ni-conjugated polymer based nanowires.

Here, we report on the development of a strategy consisting of a two-step process for preparing Ni-PPy and Ni-PEDOT nanowires with a good adhesion between the polymer and the metal. Prior to electropolymerization, the Ni surface was pretreated with a bifunctional molecule, which through specific interactions ensures a good adhesion between the two nanowires segments. In a second part, we describe the synthesis of trisegmented magnetic metal-conjugated polymer (CP)-noble metal nanowires, typically Ni-PPy-Pt and Ni-PEDOT-Au nanowires, and their structural characterization by SEM and TEM. This kind of 1D nanostructures offers various possibilities in terms of self-assembly or functionalization by using the specific surface chemistry of the different segments. Finally, for the first time, we report on the preparation of nanowires composed of a CP junction sandwiched between two magnetic segments of different nature,

* To whom correspondence should be addressed. Tel.: +32-10-472702. Fax: +32-10-451593. E-mail: sophie.demoustier@uclouvain.be.

Received for review January 11, 2010 and accepted April 12, 2010

DOI: 10.1021/am100023k

typically trisegmented Ni-CP-Co nanowires. The efficiency of the process, in particular the Ni/CP and CP/Co interfaces robustness, was checked by observing the different nanostructures by SEM and/or TEM. These fully magnetic multisegmented nanowires meet all criteria required for tunnel magnetoresistance manifestation: as good organic conductors, conjugated polymers have both relatively long spin relaxation times and a sufficient large conductivity when the multistriped geometry offers an inorganic/organic interface quality. This suitable configuration makes them very attractive candidates for fundamental investigations in organic spintronics (18−20).

EXPERIMENTAL SECTION

Materials. Polycarbonate track-etched membranes with a thickness of 21 μm, a pore density of 1×10^9 pores cm^{-2}, and an average pore size of 110 nm, supplied by it$_4$ip (http://www.it4ip.be), were used as nanoporous templates. Nickel plates consisted of silicon wafers on which Ni was thermally evaporated (thickness of the Ni layer was 20 nm). They were kept in an inert atmosphere and rapidly used after metallization. Pyrrole (Py, Acros, 99%) and 3,4-ethylenedioxythiophene (EDOT, Sigma-Aldrich) were purified immediately before use by passing them through a microcolumn constructed from a Pasteur pipet, glass wool, and activated alumina. Lithium perchlorate ($LiClO_4$, Acros), sodium dodecylsulfate (SDS, Acros), boric acid (H_3BO_3, UCB), nickel(II) sulfate hexahydrate ($NiSO_4.6H_2O$, Acros), cobalt(II) sulfate heptahydrate ($CoSO_4.7H_2O$, Sigma-Aldrich), potassium chloride (KCl, Acros), potassium hydrogenophosphate (K_2HPO_4, Acros), hydrogen tetrachloroaurate trihydrate ($HAuCl_4.3H_2O$, Sigma Aldrich, 99,9%), sodium hexachloroplatinate hexahydrate ($Na_2PtCl_6.6H_2O$, Sigma Aldrich, 98%), ferrocyanide(II) trihydrate ($K_4Fe(CN)_6.3H_2O$, Acros), and dichloromethane (CH_2Cl_2, Acros) were used without any prior purification. Deionized water was used to prepare all aqueous solutions. The iodine solution was prepared by dissolving 6 g of potassium iodide (KI, Merck) and 1.5 g of iodine (I_2, Sigma-Aldrich) in 60 mL of deionized water.

Synthesis of 3-(Pyrrol-1-yl)Propanoic Acid (3PPA) (21, 22). Twenty-five grams (0.2 mol) of *N*-(2-Cyanoethyl)-pyrrole ($C_7H_8N_2$, Acros) and 60 mL of a solution of potassium hydroxide 6.7 M were brought to reflux until the organic phase disappeared (about 5 h). To the resulting cooled amber transparent solution was added 18 mL of water. The solution was then acidified to reach a pH of 5 with hydrochloric acid 8 M. The crude product was extracted five times with diethyl ether. The resulting organic phase was dried with sodium sulfate anhydrous and evaporated under reduced pressure to lead to a beige product. Recrystallization was then carried out in hot n-heptane (90−100 °C). Nucleic magnetic resonance (NMR) was used to identify the product. NMR spectra were recorded at 300 MHz for ^{1}H and 75 MHz for ^{13}C on a Bruker Avance with a 5 mm BBFO probe gradients-z. ^{1}H NMR ($CDCl_3$): δ 2.84 (t, J = 6.9 Hz, 2H); 4.20 (t, J = 6.9 Hz, 2H); 6.15 (t, J = 2.1 Hz, 2H); 6.70 (t, J = 2.1 Hz, 2H). ^{13}C NMR ($CDCl_3$): δ 36.2 (CH_2−COOH); 44.5 (CH_2−N); 108.6 (Cβ); 120.5 (Cα).

SAM Grafting on Nickel. Self-assembled monolayers of 3-(Pyrrol-1-yl)propanoate were deposited on freshly prepared nickel plates by immersing the substrates during 18 h in aqueous solutions of 3PPA of various concentrations ranging from 2 to 250 mM. The pH of all solutions was fixed at 12 by addition of an adapted amount of NaOH (Table 1).

The electrochemical probe used to confirm the formation of a 3PPA monolayer on nickel was the Fe^{III}/Fe^{II} redox couple. The electrochemical bath contained 2.5 mM potassium ferrocyanide (II) trihydrate ($K_4Fe(CN)_6 \cdot 3H_2O$, Acros) and 0.1 M lithium perchlorate ($LiClO_4$, Acros) in deionized water.

Table 1. Composition of the Different Solutions Used for the SAM Deposit on Nickel

C_o (mM)	[NaOH] (M)
2	0.012
6	0.016
10	0.02
50	0.06
250	0.26

Preparation of Bisegmented Ni-PPy and Trisegmented Ni-PPy-Pt, Ni-PEDOT-Au, Ni-PPy-Co, and Ni-PEDOT-Co Nanowires. All electrochemical experiments were performed with a CHI660B Electrochemical Workstation (CH Inc.) in a conventional one-compartment cell at room temperature with a Pt disk counter electrode and a Ag/AgCl reference electrode. A 300 nm thick layer of gold evaporated on one side of the polycarbonate membrane served as working electrode. In these conditions of gold evaporation, the base of the nanopores is not completely blocked and has an annular shape. As reported by Lee et al., this electrode shape can strongly affect the conjugated polymer morphology, when the polymer is directly electropolymerized from the working electrode (23). However, in this work, the shape of the electrode has no impact on the resulting CP segment morphology as we always started the nanowire synthesis by electrodepositing a first long metal segment terminated by a flat top surface. All the metal/conjugated polymer nanowires were fabricated by a sequential electrodeposition of metal and polymer segments into the nanopores of a polycarbonate membrane through reduction of the corresponding metallic salt or oxidation of the corresponding monomer, respectively. The length of each material segment is controlled by the electrical charge passed through the system during the electrodeposition. Prior to each electrodeposition step, the electrodeposition solution was allowed to diffuse within the nanopores for a few minutes. After each electrodeposition step, the samples were thoroughly rinsed with deionized water. Nickel and cobalt segments were deposited from aqueous solutions containing 0.5 M H_3BO_3 and 0.85 M $NiSO_4 \cdot 6H_2O$ or 0.85 M $CoSO_4 \cdot 7H_2O$, respectively. Nickel was electrodeposited at a constant potential of −1.05 V. The electrodeposition of Co nanowires was carried out by chronoamperommetry at a potential of −0.95 V.. Electropolymerization of pyrrole was carried out by cyclic voltammetry from an aqueous solution containing 0.1 M $LiClO_4$, 0.02 M pyrrole, and 7×10^{-4} M SDS. The potential was swept between 0 and 0.85 V with a scan rate, if not specifically mentioned, of 400 mV s^{-1}. Electropolymerization of EDOT was performed by using an aqueous electrolyte containing 0.1 M $LiClO_4$ and 0.014 M EDOT, and by sweeping the potential between 0.2 and 1.1 V at a scan rate of 400 mV s^{-1}. In this work, no sodium dodecylsulfate surfactant was added to the electropolymerization bath as at the used EDOT concentration, the monomer was still soluble in pure water. Electrodeposition of Au was performed by cycling the potential of the working electrode from 0.7 to 0 V at 200 mV s^{-1} using a homemade cyanide free solution (0.1 M KCl, 0.1 M K_2HPO_4, and 0.03 M $HAuCl_4 \cdot 3H_2O$ in deionized water). Electrodeposition of Pt was accomplished potentiostatically at −0.2 V from an electrochemical bath containing 0.01 M $Na_2PtCl_6 \cdot 6H_2O$ and 0.5 M H_2SO_4 in deionized water.

Structural Analysis. The dimensions and morphology of the nanowires were studied by transmission electron microscopy (TEM) after dissolution of the PC template. TEM pictures were obtained using a LEO 922 transmission electron microscope (Carl Zeiss SMT Inc.) operating at 200 kV. After removing the evaporated gold layer with iodine solution and, dissolving the template in dichloromethane, two or three drops of the resulting nanowires suspension were placed on a carbon film grid (Agar Scientific Ltd.). Energy-dispersive X-ray spectroscopy (EDX)

Scheme 1. Schematic Representation of the Chemical Pretreatment of the Nickel Substrate with 3-(Pyrrol-1-yl) Propanoic Acid Molecules (3PPA) for the Formation of an Adherent Polypyrrole Coating

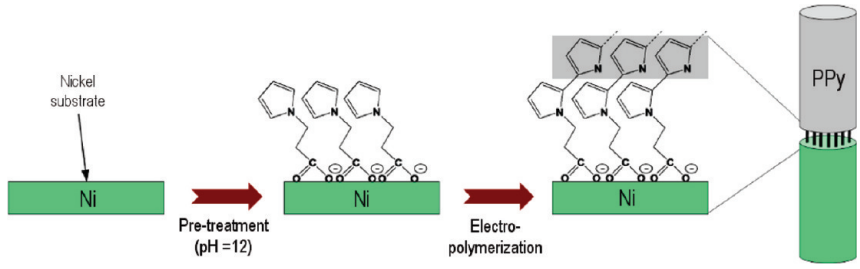

experiments were carried out with the LEO 922 TEM equipped with an INCA x-sight detector (Oxford Instruments).

RESULTS AND DISCUSSION

Synthesis of Robust Magnetic Metal-Conjugated Polymer Bisegmented Nanowires. With the aim of preparing multisegmented nanowires containing one or two magnetic metal segments, we first focus our attention on the development of a synthetic process allowing the preparation of strong Ni/CP interfaces. Our approach consists in a chemical pretreatment of the active metal substrate with an appropriate bifunctional molecule to form a passivating self-assembled monolayer (SAM) (24) that suppresses or limits the metal redissolution without preventing the electrodeposition of the CP. More precisely, for promoting the adhesion of the CP on nickel, we used 3-(Pyrrol-1-yl) propanoic acid (3PPA). This passivating molecule was chosen because of its facile synthesis (21, 22) and because it contains two end-functional groups, a carboxylate group at one extremity and a pyrrole group at the other end, that can specifically interact with the Ni substrate (25) and the growing CP, respectively. Moreover, the presence of a short alkyl chain between the two reactive groups allows the formation of well-covering monolayer without stopping further electrochemical process at the Ni electrode. As shown in Scheme 1, a molecular layer of 3PPA is chemisorbed onto the nickel surface and, as observed by others (26), the monomeric units within the molecular layer act as favorable nucleation sites for electrochemical polymerization. Very recently, Okner et al. (27) also reported on the use of this 3PPA molecule in order to improve the adhesion of polymer coating onto medical implants. However, in this work, the suggested strategy was different from the one developed in this study, as they directly coelectropolymerized 3PPA with to other pyrrole-derivatives monomers onto the metallic surface.

We first investigated the ability of forming a 3PPA monolayer onto a nickel substrate by using flat nickel substrates as model systems. The substrates were immersed for 18 h in basic aqueous solutions of 3PPA of different concentrations (see Experimental Section), rinsed abundantly with deionized water, and dried under nitrogen flux. The formation of a more or less dense layer was highlighted by cyclic voltammetry using a redox probe ($K_4Fe(CN)_6 \cdot 3H_2O$, see Figure S1 in the Supporting Information). The electrochemical activity of the redox couple Fe^{III}/Fe^{II} using different chemically modified nickel substrates as working electrodes was followed by sweeping the potential between 0 and 0.5 V. From this study, it clearly appears that increasing the [3PPA] in the pretreatment solution leads to an increased gap (ΔE) between the oxidation and reduction peak potentials of the redox couple Fe^{III}/Fe^{II} (Table 2). This transition toward a less-reversible system can be explained by the decrease of the electron transfer rate, resulting from the grafting of a progressively denser 3PPA monolayer onto the Ni electrode. This was confirmed by X-ray photoelectron spectroscopy showing the disappearance of the peak assigned to metallic Ni and the appearance of a nitrogen peak in the XPS spectrum when Ni plates were chemically treated with 3PPA molecules (see Figure S3 in the Supporting Information).

Table 2. Evolution of the Anodic Peak (E_A), Cathodic Peak (E_C), and $\Delta E = E_A - E_C$ of the Redox Probe Fe^{III}/Fe^{II} as a Function of the [3PPA] Used for the Formation of a SAM onto the Ni Electrode

[3PPA] (mM)	E_A (mV)	E_C (mV)	ΔE (mV)
0 (bare Ni)	389	225	164
2	403	220	183
6	403	220	183
10	428	215	213
50	473	203	270

Membrane-based technology has already been successfully used to fabricate nanowires of magnetic metals such as Ni and Co (28−30). Here, we used this template electrochemical method for preparing smooth, homogeneous and narrow Ni nanowires (Figure 1a, b). Nickel was electrodeposited by chronoamperommetry at $E = -1.05$ V within the pores of a polycarbonate membrane ($\Phi = 110$ nm) from an electrochemical bath containing Ni sulfate hexahydrate ($NiSO_4 \cdot 6H_2O$) and boric acid (H_3BO_3) (31). The length of the Ni nanowires can be easily tuned by the electrodeposition time (Figure 1c).

Assuming that the chemical pretreatment of Ni by 3PPA molecules is also efficient in confined environment, the adhesion of the conjugated segment onto Ni nanowires should depend on the homogeneity and compactness of the deposited monolayer. To determine the optimal [3PPA] to be used for the formation of a SAM that will efficiently slow down the oxidation and redissolution of the nickel without stopping the electropolymerization process, we carried out pyrrole electropolymerization on Ni nanowires that were previously treated with 3PPA solutions of four different

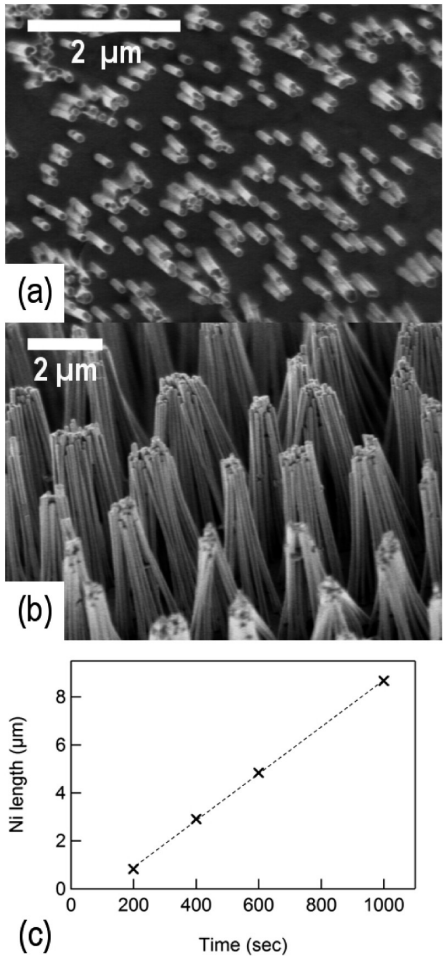

FIGURE 1. (a, b) SEM pictures of Ni nanowires after dissolution of the template membrane: (a) electrodeposition time = 200 s ($L_{Ni} \approx$ 800 nm), (b) electrodeposition time = 600 s ($L_{Ni} \approx 5\ \mu$m). (c) Length of the Ni nanowires as a function of electrodeposition time.

concentrations, 2, 10, 50, and 250 mM. In all cases, Ni nanowires embedded in the PC membrane were immersed in the 3PPA solution for 18 h. An aqueous solution containing 0.02 M pyrrole and 7×10^{-4} M sodium dodecylsulfate (SDS) was then used for the electrosynthesis of the polymer. According to the length calibration curve presented in Figure 1c, 8−0 μm long nickel nanowires were prepared. PPy nanowires were deposited by sweeping the potential between 0 and 0.85 V at a scan rate of 400 mV s^{-1} during 1000 cycles. The morphological observations performed by TEM on this series of samples are gathered in Figure 2.

When the electropolymerization of pyrrole was carried out on bare nickel nanowires, only one-component PPy nanowires and one-component Ni nanowires were found, but no bisegmented Ni-PPy nanowires (Figure 2a, b). This observation results from the Ni oxidation and partial redissolution mainly occurring at the beginning of the polymer electrosynthesis and, leading to the formation of very fragile Ni/PPy interfaces. Consequently, all nanowires break at the metal/polymer interface. When using a 2 or 10 mM 3PPA solution for the formation of a SAM on the top of the Ni nanowires prior to pyrrole electropolymerization, a few entire Ni-PPy nanowires are obtained, but in most cases, with very short PPy segments bound to Ni nanowires (Figure 2c, d). Furthermore, a large number of one-component nanowires are still present, demonstrating the weakness of the formed metal/polymer interface. By increasing the [3PPA] up to 50 mM, a much larger number of unbroken Ni-PPy bisegmented nanowires are recovered (Figure 2e, f). As a further increase in the [3PPA] (up to 250 mM) does not lead to any significant improvement of the PPy adherence, we decided to use a 3PPA concentration of 50 mM for monolayer deposition in the next experiments.

To show the ability of the 3PPA monolayer in reducing the nickel oxidation and redissolution occurring at the positive potentials applied for polymer formation, pyrrole electropolymerization on bare and chemically pretreated nickel nanowires was followed, at different steps of the process, by cyclic voltammetry (Figure 3). In the first cycle recorded during pyrrole electropolymerization on bare Ni nanowires, nickel oxidation starts at a potential located around +0.3 V. In the following potential sweeping cycles, metal oxidation appears at a slightly higher potential (∼ + 0.5 V), indicating the formation of an oxide layer that partially passivates the Ni electrode toward oxidation but does not completely suppress it. As a consequence, the interface with PPy is based on metal oxide—polymer mixture, which leads to a very poor adhesion between PPy and Ni and consequently to the formation of broken nanowires, as preceedingly revealed by TEM (Figure 2a, b). For comparison, the CV curves recorded during electropolymerization of pyrrole onto 3PPA pretreated Ni segments are presented in Figure 3b. Though in the first cycle, a weak nickel oxidization peak (lower oxidation current than on bare Ni) still appears at a potential around +0.5 V, the phenomenon is no more observed during the following cycles. Moreover, in this case, the CV cycles look like typical $I-V$ curves recorded during electropolymerization of pyrrole on noble metals.

We also compared the CV curves recorded during polymer electrosyntheses on top of various pretreated nickel surfaces (see Figure S2 in the Supporting Information) and, found that the SAM compactness has a significant influence on pyrrole electropolymerization rate. Indeed, by increasing the homogeneity and compactness of the organic barrier onto the Ni segment, nickel oxidation and redissolution is strongly hindered and consequently, PPy growth is faster. This trend can be correlated with the TEM observation that the length of PPy segment increases with increasing [3PPA] used during the chemical pretreatment of the Ni nanowire top surface, while keeping all the other synthesis parameters constant.

Though the electropolymerization conditions were even more drastic (potential sweeping up to 1.1 V vs Ag/AgCl), 3,4-ethylenedioxythiophene (EDOT) was also successfully electropolymerizd on chemically pretreated Ni nanowires (see Figure S4 in the Supporting Information).

Synthesis of Magnetic Ni-CP-Noble Metal Trisegmented Nanowires. With the aim of producing trisegmented nanowires containing one magnetic segment, we considered the synthesis of two types of nanostructures:

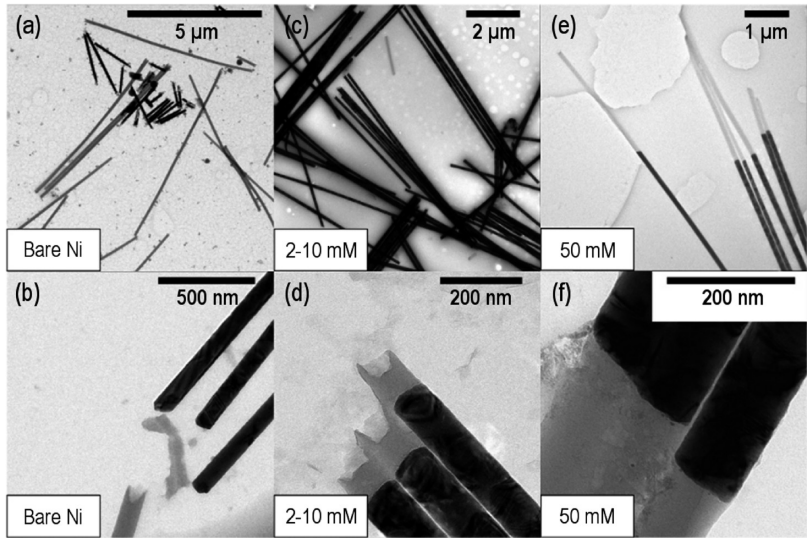

FIGURE 2. TEM images of Ni-PPy nanowires synthesized using different [3PPA] for the SAM deposition et the interface.

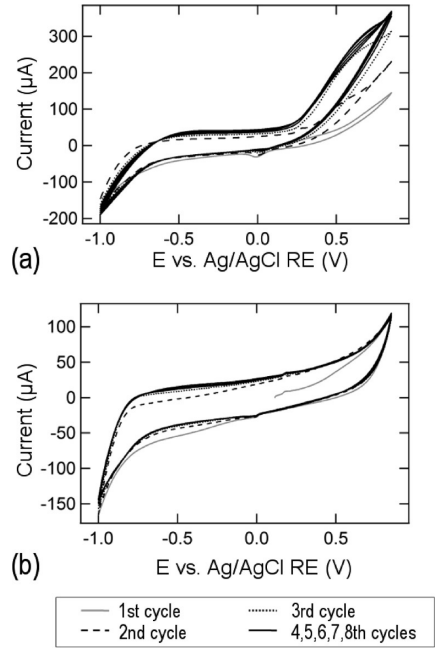

FIGURE 3. Cyclic voltammograms recorded during electropolymerization of pyrrole on (a) 90 nm diameter bare Ni nanowires, (b) 3PPA-modified Ni nanowires. Scan rate $=50$ mV s^{-1}.

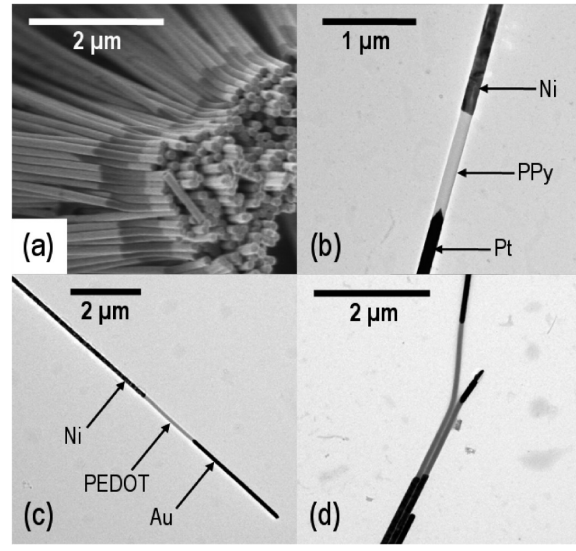

FIGURE 4. (a) SEM picture of 110 nm diameter trisegmented Ni-PPy-Pt nanowires. (b) TEM picture of a 110 nm diameter trisegmented Ni-PPy-Pt nanowire. (c, d) TEM pictures of Ni-PEDOT-Au nanowires with a straight polymer junction (c) and a bent polymer junction (d).

Ni-PPy-Pt and Ni-PEDOT-Au nanowires. This choice was based on the observed preferential affinities between PPy and Pt and between PEDOT and Au. As previously reported, for the upper metal-onto-polymer interfaces, no chemical pretreatment was required to get mechanically strong interfaces (13, 14). The resulting Ni-PPy-Pt and Ni-PEDOT-Au nanostructures were characterized by SEM and TEM. As shown in Figure 4, entire nanowires are formed for both types of nanostructures. Trisegmented nanowires including polymer and metal segments of various lengths were then prepared. When the length of the conjugated polymer segment and the top noble metal segment are increased, the chemically modified Ni/CP interface is subjected to increasing strain. This leads for Ni-PPy-Pt nanostructures to the breaking of the bottom magnetic metal/polymer interface, while the Ni/PEDOT interfaces withstand this strain and, entire long Ni-PEDOT-Au nanowires can be prepared (Figure 4c). This higher strength of the Ni/PEDOT interfaces might be due to the larger flexibility of PEDOT segments that leads to their easier ability of bending (as illustrated in Figure 4d), compared to PPy-based nanowires.

Synthesis of Magnetic Ni-CP-Co Trisegmented Nanowires. On the basis of the promising results obtained on Ni-CP-Noble metal nanowires, our next objective was to adapt the process for preparing magnetic metal−organic conjugated polymer based nanowires, presenting new physical interesting properties. More specifically, we aimed at the preparation of trisegmented nanowires containing a very short polymer junction sandwiched between two different magnetic segments, typically Ni-CP-Co nanowires.

To obtain a magnetoresistance effect in these trisegmented nanostructures, all three components have to satisfy some length requirements, as illustrated in Scheme 2: a long

Scheme 2. (a) Schematic Representation of the Aimed tri-Segmented Ni-CP-Co Nanowire Architecture. (b) Principle of the Magnetoresistance Effect Expected in These Trisegmented Ni-CP-Co Nanowires

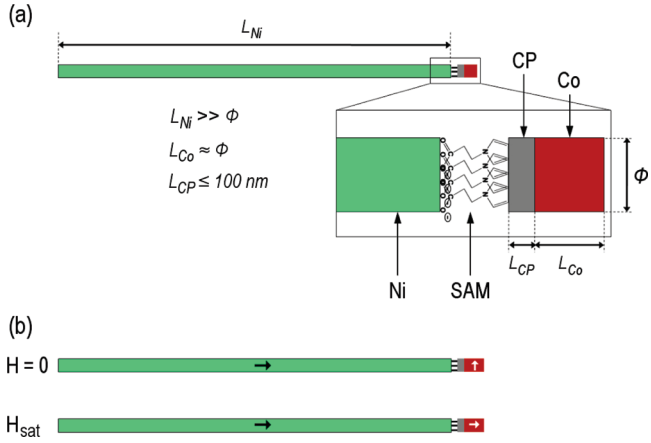

Ni segment to get a magnetization of type "form", directed along the axis of the nanowire, a short organic junction (length ≤100 nm) to mediate the spin-polarized signal, and a short Co segment (length ≈ nanowire diameter) with a magnetization of type "magnetocrystalline", directed perpendicular to the axis of the nanowire. In this configuration, the following expected magneto-resistance effect should occur: at zero magnetic field ($H = 0$), the current does not cross the organic junction, but applying a magnetic field ($H = H_{sat}$) aligns the magnetization of Co along the axis of the nanowire and consequently, strongly decreases the resistance of the system (Scheme 2b). First, in order to evaluate the feasibility of preparing such hybrid nanostructures, trisegmented nanowires with magnetic metal and polymer segments of different lengths were prepared. First, a Ni segment was electrodeposited into the nanopores of a polycarbonate membrane and its top surface was covered by a SAM of 3PPA molecules, under the optimized conditions described previously (SAM was formed from a 50 mM 3PPA solution). Then a conjugated polymer (either PPy or PEDOT) was electrodeposited onto this Ni-modified surface, and finally, a top cobalt segment was electroplated. SEM and TEM pictures of typical resulting nanostructures are gathered in Figure 5.

The SEM picture in Figure 5a shows a bundle of PPy-based nanostructures with some entire trisegmented Ni-PPy-Co nanowires, but a majority of bisegmented Ni-PPy nanowires. TEM picture in Figure 5b confirms what was largely observed for Ni-PPy-Co nanowires: breaking always occurs at the PPy/Co interfaces, and never at the Ni/PPy ones. The situation was quite different when using PEDOT as CP segment. Indeed, even with long PEDOT segments, entire Ni-PEDOT-Co nanowires were observed (Figure 5c). On this figure, corresponding to a TEM image of a freshly prepared Ni-PEDOT-Co nanowire sample (TEM observation made on the day of the synthesis), the electronic contrast between the cobalt and the polymer is sufficiently high to easily distinguish both materials. However, when observing the same sample 10 days after the synthesis (TEM pictures of Figure 6), it was much more difficult to unambiguously distinguish the Co and the PEDOT segments.

This lost of contrast, accompanied by the apparition of dark "spheres", as illustrated in Figure 6, results from the fast oxidation and degradation of Co when kept in air. In order to confirm the segmented composition of the nanowires, we performed TEM-EDX analysis. As illustrated in Figure 6, EDX reveals the presence of the characteristic element for each of the three segments (Ni, S for PEDOT, and Co). The traces of sulfur and chlorine found in the Co segment are probably due to the formation of Co complexes with sulfate and chlorine ions, coming from cobalt and PEDOT electroplating solutions, respectively.

The final step in the elaboration of the Ni-CP-Co nanowires was to reduce the length of the cobalt segment and of the polymer junction in order to fit with the aimed architecture presented in Scheme 2. To produce polymer junctions of very short length, we reduced the PPy growth rate by increasing the potential scan rate applied during the electropolymerization. This electrosynthesis parameter change has two interesting effects. On the one hand, it allows obtaining nanowires of more uniform length, and on the other hand, it leads to the formation of a rather flat upper part of the polymer junction instead of the meniscus shape previously observed. So, by sweeping the potential at 800 mV s^{-1} instead of 400 mV s^{-1}, and by adjusting the number of potential cycles, we succeeded, for the first time, to prepare entire Ni-PPy-Co nanowires presenting a very short polymer junction (of about only 20 nm length) and, without any short circuit (Figure 7).

The Co segments were synthesized by chronoamperometry at a constant applied potential of −0.95 V. Upon these synthesis conditions, the growing of Co nanostructures was rather fast, the growth rate of Co nanowire in nanopores of 110 nm being estimated to be about 12 nm s^{-1}. Despite this fast Co growth rate, it was however possible to prepare relatively short Co segments by reducing the time of electroplating to only a few seconds. As illustrated on the TEM picture of Figure 7, we succeeded up to now to grow Co segments of about 300 nm length on top of the short PPy junction. The study of the magnetoresistance properties of these trisegmented Ni-PPy-Co having the right architecture is now considered. As Co is unstable in air (see Figure 6), we are currently starting this investigation on nanowires still embedded into the polycarbonate template.

CONCLUSIONS

In this work, we present the use of a template-based method for the electrochemical synthesis of new magnetic-conjugated polymer nanowires of controlled dimensionality through the sequential synthesis of the multiple segments. To deposit PPy and PEDOT onto an active metal such as Ni and get mechanically robust metal/polymer interfaces, we developed a strategy consisting in a two-step process. Prior to the polymer electropolymerization, an organic monolayer of 3PPA was deposited on the Ni surface. Though the process

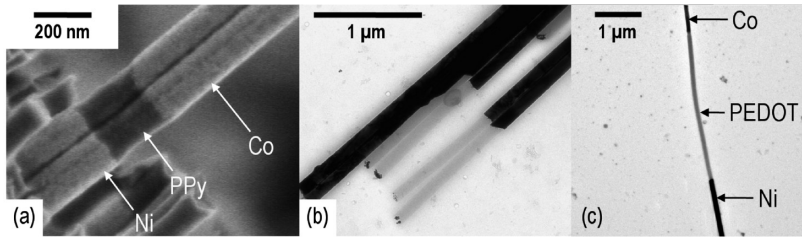

FIGURE 5. (a) SEM pictures of 110 nm diameter Ni-PPy-Co nanowires. (b) TEM picture of 110 nm diameter Ni-PPy-Co broken at the PPy/Co interfaces. (c) TEM picture of a 110 nm diameter Ni-PEDOT-Co nanowire.

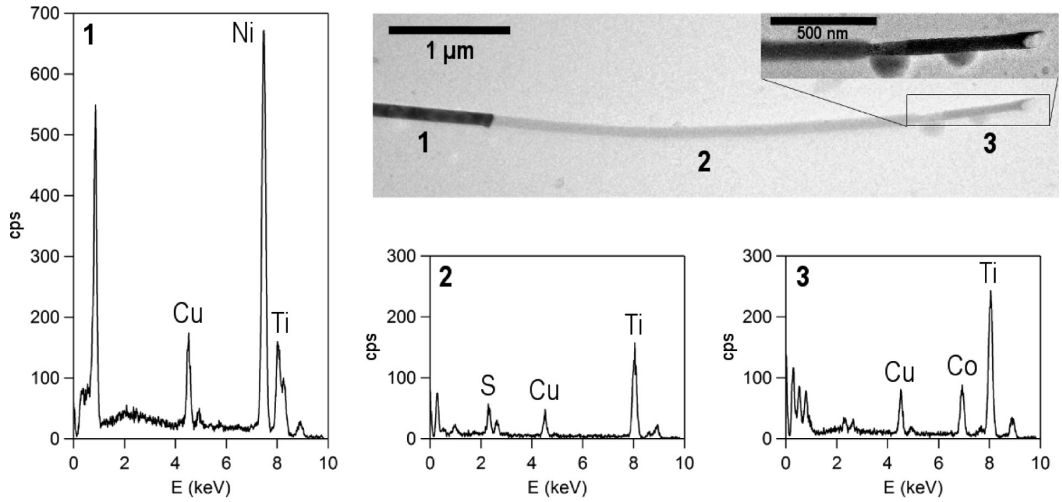

FIGURE 6. EDX spectra recorded on each segment of a $\Phi = 110$ nm trisegmented nanowire. Only the Kα X-rays of the elements that identify each material are indicated. The presence of Ti and Cu elements with Kα X-rays at 4.5 and at 8 keV comes from the titanium holder and the copper grid. The TEM image shows the analyzed trisegmented nanowire with a zoom on the cobalt segment.

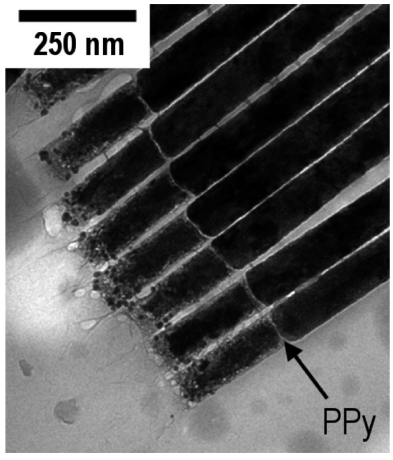

FIGURE 7. TEM picture of Ni-PPy-Co nanowires with a very short polymer junction and a short Co segment.

could still be improved, it already allows, as proved by SEM and TEM analyses, the successful preparation of a series of magnetic-conjugated polymer based nanostructures, typically Ni-PPy-Pt, Ni-PEDOT-Au, Ni-PPy-Co, and Ni-PEDOT-Co trisegmented nanowires. All these multicomponent nanostructures present interesting potential applications. On the one hand, Ni-conjugated polymer-noble metal nanowires, where each segment possesses unique physical and chemical properties (the noble metal offers excellent conductivity, the conjugated polymer brings stimuli-sensitivity, and the ferromagnetic nickel segment imparts the possibility to magnetically position and align the nanowires on a device) could be useful multifunctional nanostructures in the field of biosensors. On the other hand, the successful synthesis of trisegmented Ni-PPy-Co nanowires with a very short PPy junction and a small Co segment are very interesting nanostructures with potential applications in the field of organic spintronics. These studies are currently under progress.

Acknowledgment. The authors thank Etienne Ferain and it$_4$ip company for supplying polycarbonate membranes, Pascale Lipnik for her assistance in performing the TEM-EDX analysis, and Luc Piraux for helpful discussions about spintronics. The work was supported by the 'Communauté française de Belgique' (Action de recherche concertée, NANOMOL), by the Belgian Science Policy through the Interuniversity Attraction Pole Program (P6/27) and, by the Wallonia Region (NANOTIC program). S.D.C. thanks the F.R.S.-FNRS for its Senior Research Associate position.

Supporting Information Available: More details about the characterization by electrochemical methods and X-ray photoelectron spectroscopy of the self-assembled monolayer of 3PPA molecules formed on Ni plane substrate and on Ni nanowires (PDF). This material is available free of charge via the Internet at http://pubs.acs.org.

REFERENCES AND NOTES

(1) Kovtyukhova, N. I.; Mallouk, T. E. *Chem.—Eur. J.* **2002**, *8*, 4354–4363.
(2) Bangar, M. A.; Hangarter, C. M.; Yoo, B.; Rheem, Y.; Chen, W.; Mulchandani, A.; Myung, N. V. *Electroanalysis* **2008**, *21*, 61–67.

(3) Martin, B. R.; Dermody, D. J.; Reiss, B. D.; Fang, M.; Lyon, L. A.; Natan, M. J.; Mallouk, T. E. *Adv. Mater.* **1999**, *11*, 1021–1025.
(4) Park, S.; Chung, S.-W.; Mirkin, C. A. *J. Am. Chem. Soc.* **2004**, *126*, 11772–11773.
(5) Hurst, S. J.; Payne, E. K.; Qin, L.; Mirkin, C. A. *Angew. Chem., Int. Ed.* **2006**, *45*, 2672–2692.
(6) Liu, R.; Lee, S. B. *J. Am. Chem. Soc.* **2008**, *130*, 2942–2943.
(7) Wang, X.; Ozkan, C. S. *Nano Lett.* **2008**, *8*, 398–404.
(8) Cao, Y.; Kovalev, A. E.; Xiao, R.; Kim, J.; Mayer, T. S.; Mallouk, T. E. *Nano Lett.* **2008**, *8*, 4653–4658.
(9) Lorcy, J. M.; Massuyeau, F.; Moreau, P.; Chauvet, O.; Faulques, E.; Wéry, J.; Duvail, J. L. *Nanotechnology* **2009**, 405601.
(10) Banerjee, P.; Perez, I.; Henn-Lecordier, L.; Lee, S. B.; Rubloff, G. W. *Nat. Nanotechnol.* **2009**, *4*, 292–296.
(11) Liu, R.; Duay, J.; Lane, T.; Lee, S. B. *Phys. Chem. Chem. Phys.* **2010**; DOI: 10.1039/b918589p.
(12) Zhang, C.; Grander, J.; Liu, R.; Lee, S. B.; Eichhorn, B. W. *Phys. Chem. Chem. Phys.* **2010**; DOI: 10.1039/b918587a.
(13) Gence, L.; Faniel, S.; Gustin, C.; Melinte, S.; Bayot, V.; Callegari, V.; Reynes, O.; Demoustier-Champagne, S. *Phys. Rev. B* **2007**, *76*, 115415−1115415−8.
(14) Callegari, V.; Gence, L.; Melinte, S.; Demoustier-Champagne, S. *Chem. Mater.* **2009**, *21*, 4241–4247.
(15) Zalewska, T.; Lisowska-Oleksiak, A.; Biallozor, S.; Jasulaitiene, V. *Electrochim. Acta* **2000**, *45*, 4031–4040.
(16) Lallemand, F.; Auguste, D.; Amato, C.; Hevesi, L.; Delhalle, J.; Mekhalif, Z. *Electrochim. Acta* **2007**, *52*, 4334–4341.
(17) Lallemand, F.; Plumier, F.; Delhalle, J.; Mekhalif, Z. *Appl. Surf. Sci.* **2008**, *254*, 3318–3323.
(18) Pramanik, S.; Stefanita, C.-G.; Patibandla, S.; Bandyopadhyay, S.; Garre, K.; Harth, N.; Cahay, M. *Nat. Nanotechnol.* **2007**, *2*, 216–219.
(19) Naber, W. J. M.; Faez, S.; van der Wiel, W. G. *J. Phys. D Appl. Phys.* **2007**, *40*, R205–R228.
(20) Sanvito, S. *Nat. Mater.* **2007**, *6*, 803–804.
(21) Maeda, S.; Corrada, R.; Armes, S. P. *Macromolecules* **1995**, *28*, 2905–2911.
(22) Roux, S.; Audebert, P.; Pagetti, J.; Roche, M. *New J. Chem.* **2000**, *24*, 877–884.
(23) Cho, S. I.; Lee, S. B. *Acc. Chem. Res.* **2008**, *41*, 699–707.
(24) Mekhalif, Z.; Delhalle, J.; Lang, P.; Garnier, F.; Pireaux, J.-J. *Synth. Met.* **1998**, *96*, 165–175.
(25) Wulser, K. W.; Langell, M. A. *Catal. Lett.* **1992**, *15*, 39–50.
(26) Rider, D. A.; Harris, K. D.; Wang, D.; Bruce, J.; Fleischauer, M. D.; Tucker, R. T.; Brett, M. J.; Buriak, J. M. *ACS Appl. Mater. Interfaces* **2009**, *1*, 279–288.
(27) Okner, R.; Shaulov, Y.; Tal, N.; Favaro, G.; Domb, A. J.; Mandler, D. *ACS Appl. Mater. Interfaces* **2009**, *1*, 758–767.
(28) Whitney, T. M.; Jiang, J. S.; Searson, P. C.; Chien, C. L. *Science* **1993**, *261*, 1316–1319.
(29) Ferré, R.; Ounadjela, K.; George, J. M.; Piraux, L.; Dubois, S. *Phys. Rev. B* **1997**, *56*, 14066.
(30) Narayanan, T. N.; Shaijumon, M. M.; Ci, L.; Ajayan, P. M. *Nano. Res.* **2008**, *1*, 465–473.
(31) Piraux, L.; Encinas, A.; Vila, L.; Mátéfi-Tempfli, S.; Mátéfi-Tempfli, M.; Darques, M.; Elhoussine, F.; Michotte, S. *J. Nanosci. Nanotechnol.* **2005**, *5*, 372–389.

AM100023K